

**PAPER**

Improving SPDC single-photon sources via extended heralding and feed-forward control

OPEN ACCESS**RECEIVED**

25 January 2019

REVISED

20 April 2019

ACCEPTED FOR PUBLICATION

2 May 2019

PUBLISHED

29 May 2019

Marcello Massaro , Evan Meyer-Scott, Nicola Montaut, Harald Herrmann and Christine Silberhorn 

Integrated Quantum Optics, University of Paderborn, Warburger Str. 100, D-33098 Paderborn, Germany

E-mail: marcello.massaro@upb.com**Keywords:** single-photon sources, feed-forward, spectral filtering, spdc

Original content from this work may be used under the terms of the [Creative Commons Attribution 3.0 licence](https://creativecommons.org/licenses/by/4.0/).

Any further distribution of this work must maintain attribution to the author(s) and the title of the work, journal citation and DOI.

**Abstract**

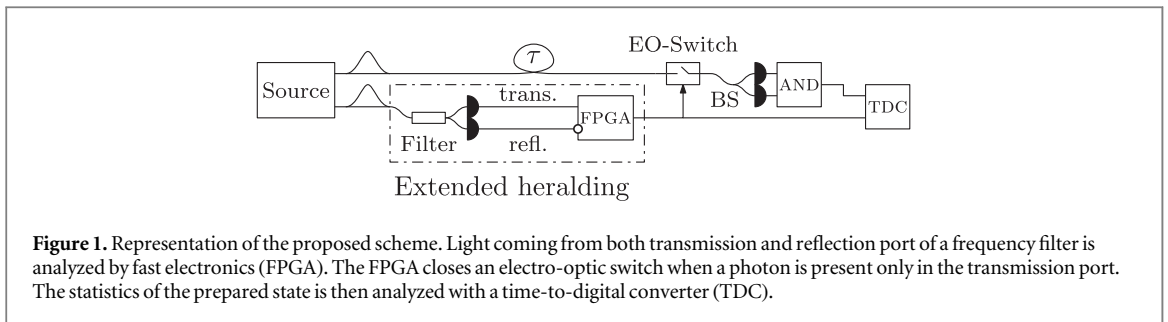
Evolving photonic quantum technologies and applications require higher and higher rates of single photon generation. In parallel, it is required that these generated photons are kept spectrally pure for multi-photon experiments and that multi-photon noise be kept to a minimum. In spontaneous parametric down-conversion sources, these requirements are conflicting, because spectral filtering to increase spectral purity always means lowering the rate at which photons are generated, and increasing the pump power means increasing the multi-photon noise. In this paper, we present a scheme, called extended heralding, which aims to mitigate the reduction of single-photon generation rate under spectral filtering by removing cases where we detect light in the rejection band of the heralding photon's filter. Our experiment shows that this allows for higher single-photon generation rates with lower multi-photon noise than the standard approach of neglecting modes falling out of the filter bandwidth. We also show that by using active feed-forward control based on this extended heralding, it is possible to further improve the performance of the original source by physically eliminating uncorrelated photons from the output stream.

1. Introduction

Many important tasks in optical quantum information processing, like boson sampling [1–3], linear optics quantum computing [4, 5], and quantum networking [6, 7], require the generation of single-photon states at high rates and with high purity. Current methods for single-photon generation include parametric downconversion (PDC) processes in nonlinear crystals and waveguides [8, 9], four-wave mixing in optical fibers and waveguides [10–12], and quantum dots [13–15] and color centers [16–18] in solid state lattices.

Although all of these technologies are able to produce single photons, the *de facto* standard in applications is still PDC sources based on nonlinear crystals, due the proven technology behind their manufacturing processes and simple operation. They are also compact, able to produce photon states of high spectral purity and indistinguishability [19, 20] and easy to package in integrated, room-temperature devices [21, 22]. These sources (called HSPS, or heralded single photon sources) produce photons in pairs, giving the user the opportunity to herald the presence of one photon by detecting its twin.

To obtain spectrally pure photons suitable for interference with other photons, two choices are possible: specifically engineering the HSPS itself in order to ensure pure photons from the beginning [23], or filtering a spectrally-correlated source [24]. Often, spectral filtering is the simpler way to obtain a pure, uncorrelated spectrum. On the other hand, these being *single* photon sources, we want to keep the noise due to multi-photon components to a minimum. To avoid such noise, it is common to pump HSPSs at low power levels, such that the probability of producing a single pair is small ($p < 0.1$). While this reduces the multi-photon component noise, it also reduces the number of 'useful events' per system-cycle (heralding rate), because most of the time no pairs will be produced. The heralding rate drops even more when spectrally pure single photons are required, since filtering in the heralding arm inevitably suppresses parts of the source output. Increasing the pump power to recover the 'lost' heralding rate will then introduce substantial multi-photon noise, such that simply increasing



the pump power is not a viable solution. This is because the filter is applied only to the heralding arm to maintain high heralding efficiency of the heralded photon [25], and light which is outside the filter in the heralding arm does not lead to heralding events. Nevertheless, it still exists in the heralded arm, leading to extra noise. Loosely, the heralding rate goes with p_f , the filtered photon production probability, while the noise in the heralding arm depends on $p(>p_f)$, the original production probability before filtering.

To improve the single photon generation rate of these sources while keeping the noise low, multiple strategies can be used. A difficult but promising approach is multiplexing, where multiple sources are combined together with feedforward switching to improve the rate of single photon generation without increasing the noise. Common schemes are spatial multiplexing [26, 27], time multiplexing [28] and frequency multiplexing [29, 30].

While these are encouraging results, they usually come with a large hardware overhead and additional setup complexity and losses when compared to single sources. To avoid these drawbacks other methods can be used to achieve better performance in certain metrics from a single SPDC source. For example, a combination of high pump repetition rate and spectral filtering has been used [31] to increase the generation rate of single-photons. Alternatively, photon-number-resolving detection can be used to eliminate higher order photon contributions, decreasing the multi-photon noise [32, 33].

Note however, when the herald photon is filtered, many unheralded photons are sent to the heralded arm. Some systems cannot rely on postprocessing alone to eliminate these unheralded photons, due to their sensitivity on incoming photon flux (e.g. detection systems based on transition edge sensors [34]). In this case, active feed-forward and electro-optical switches provide a solution, only opening the path to the heralded detector after the herald photon has been detected [35–37]. This approach uses off-the-shelf telecom equipment and thus relies on proven, cost-effective technology only.

In this paper, we present a scheme which ensures high spectral and photon-number purity of the generated state by conditioning on heralding events both within and outside the filter bandwidth, and add to this an active feed-forward strategy that physically removes unwanted photons. Our method does not pollute the heralded arm of the PDC state with noise photons and constrains the photon flux to a minimum for single-photon sensitive applications. We compare our scheme with the case of standard passive spectral filtering and measure the reduction in the noise due to our removal of higher order photon number contributions. A measure of this noise is given by the heralded second order correlation function ($g_h^{(2)}(0)$) and we register a maximum improvement of 21%, limited by losses in the heralding arm.

2. Theory and simulations

For the best heralding efficiency, often only the heralding photon is filtered. This can still project the heralded photon into a single spectral mode as long as the filter is tight enough [25]. A problem arises if the modes which the filter removes in the heralding arm are still present in the heralded arm, leading to uncorrelated noise. In particular highly multi-mode PDC states with strong spectral correlations, which are typical for standard waveguide sources, require significant filtering to achieve spectral purity and are strongly affected by this pollution. To counteract this shortcoming we introduce the concept of *extended heralding* (figure 1). Here we exploit the additional information gained by detecting not only the transmitted light of filter in the heralding arm, but also the rejected part of the spectrum which is normally discarded. We use the additional information present in the reflected heralding mode to improve the photon statistics of the heralded mode, namely by discounting events where a photon is detected in both transmitted and reflected ports, reducing multi-photon events. We follow the description of [33] with the addition of filtering and extended heralding, comparing the fidelity of the heralded state to a single photon in a single spectral mode, versus the probability of heralding. Here we take the fidelity of the heralded state before any losses, which is thus an upper limit to the fidelity achievable in practice.

2.1. Effect of filtering on fidelity

We begin with a PDC state with a certain distribution of spectral modes given by the Schmidt decomposition of the total state, where we assume the pump power is low enough to neglect time-ordering effects [38]. The state in terms of these broadband modes is [33]

$$|\psi\rangle = \bigotimes_{k=0}^{\infty} \text{sech}(q_k) \sum_{n=0}^{\infty} \tanh^n(q_k) |n_k^{(s)}, n_k^{(i)}\rangle. \quad (1)$$

This means, for each spectral-temporal Schmidt mode k in the tensor product, there is a sum in photon number from 0 to ∞ , with a thermal distribution. The squeezing parameters are defined as $q_k = B\lambda_k$, where B is an overall pump power factor, and λ_k are the eigenvalues of the Schmidt decomposition of the joint spectral amplitude. In practice the tensor product and sum need not be carried to infinity; we use a maximum of 20 spectral modes and 6 photons in simulation.

The spectral filter in the heralding (signal) arm rearranges the spectral modes. It suffices in most cases to take new (pseudo-)Schmidt decompositions of the joint spectral amplitudes transmitted and reflected by the filter [39, 40], without renormalizing. Then the state, with components now labeled t for transmitted through the filter and r for reflected, is

$$|\psi\rangle = \bigotimes_{k_t=0}^{\infty} \text{sech}(q_{k_t}) \sum_{n=0}^{\infty} \tanh^n(q_{k_t}) |n_{k_t}^{(s)}, n_{k_t}^{(i)}\rangle \bigotimes_{k_r=0}^{\infty} \text{sech}(q_{k_r}) \sum_{n=0}^{\infty} \tanh^n(q_{k_r}) |n_{k_r}^{(s)}, n_{k_r}^{(i)}\rangle, \quad (2)$$

where now the squeezing parameters are $q_{k_t} = B_t \lambda_{k_t}$ and $q_{k_r} = B_r \lambda_{k_r}$, and B_r and B_t come from the relative intensities of the transmitted and reflected modes.

We can sort the terms according to photon number as

$$|\psi\rangle = \prod_{k_t} \text{sech}(q_{k_t}) \left(|0_t\rangle + \sum_{k_t} \tanh(q_{k_t}) |1_{k_t}^{(s)}; 1_{k_t}^{(i)}\rangle + \sum_{k_t \leq k'_t} \tanh(q_{k_t}) \tanh(q_{k'_t}) |1_{k_t}^{(s)}, 1_{k_t}^{(s)}; 1_{k_t}^{(i)}, 1_{k'_t}^{(i)}\rangle \dots \right) \otimes \prod_{k_r} \text{sech}(q_{k_r}) \left(|0_r\rangle + \sum_{k_r} \tanh(q_{k_r}) |1_{k_r}^{(s)}; 1_{k_r}^{(i)}\rangle + \sum_{k_r \leq k'_r} \tanh(q_{k_r}) \tanh(q_{k'_r}) |1_{k_r}^{(s)}, 1_{k_r}^{(s)}; 1_{k_r}^{(i)}, 1_{k'_r}^{(i)}\rangle \dots \right), \quad (3)$$

and continuing with higher number terms. Then we apply a detector (insensitive to the spectral-temporal modes) on the heralding (transmitted) mode, given by the heralding projector

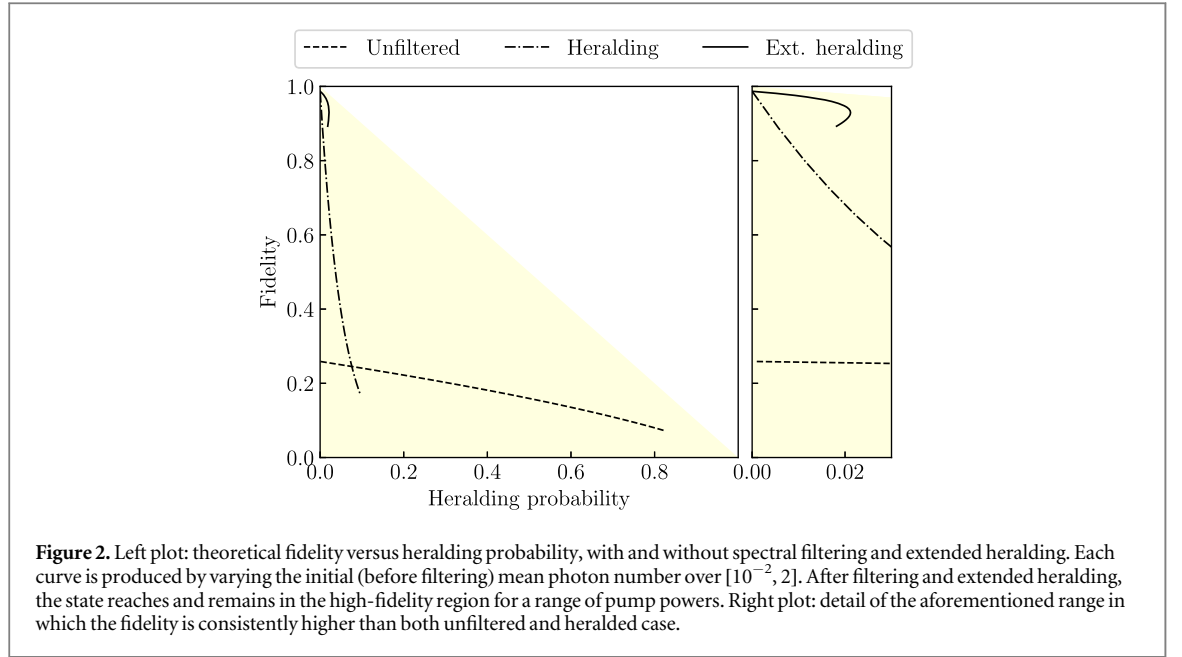
$$\hat{\Pi}_t = c_0 |0\rangle \langle 0| + c_1 \sum_{k_t} |1_{k_t}\rangle \langle 1_{k_t}| + c_2 \sum_{k_t \leq k'_t} |1_{k_t}, 1_{k'_t}\rangle \langle 1_{k_t}, 1_{k'_t}| + \dots, \quad (4)$$

where $c_{n_t} = 1 - (1 - \eta_t)^{n_t}$ is the click probability given n_t photons for detection efficiency η_t . The extended heralding (reflected mode) projector is then $\hat{\Pi}_r = \hat{1} - \hat{\Pi}_t$. This is equivalent to $\hat{\Pi}_t$, with the detection probabilities c_{n_t} replaced by the probabilities of no click, $c_{n_r} = (1 - \eta_r)^{n_r}$. Dark counts can be added to either detector with a constant term in the c_n .

Projecting the transmitted and reflected modes with their respective heralding and extended heralding detectors returns the (normalized) heralded signal state

$$\rho_s = \frac{\prod_{k_t} \text{sech}^2(q_{k_t})}{P_{\text{herald}}} \left(c_0 |0_t\rangle \langle 0_t| + c_1 \sum_{k_t} \tanh^2(q_{k_t}) |1_{k_t}\rangle \langle 1_{k_t}| + c_2 \sum_{k_t \leq k'_t} \tanh^2(q_{k_t}) \tanh^2(q_{k'_t}) |1_{k_t}, 1_{k'_t}\rangle \langle 1_{k_t}, 1_{k'_t}| + \dots \right) \otimes \frac{\prod_{k_r} \text{sech}^2(q_{k_r})}{P_{\text{ext}}} \left(c_0 |0_r\rangle \langle 0_r| + c_1 \sum_{k_r} \tanh^2(q_{k_r}) |1_{k_r}\rangle \langle 1_{k_r}| + c_2 \sum_{k_r \leq k'_r} \tanh^2(q_{k_r}) \tanh^2(q_{k'_r}) |1_{k_r}, 1_{k'_r}\rangle \langle 1_{k_r}, 1_{k'_r}| + \dots \right). \quad (5)$$

The probabilities of heralding and extended heralding (i.e. getting a click in the transmitted arm, and *no* click in the reflected arm, respectively) are



$$p_{\text{herald}} = \prod_{k_r} \text{sech}^2(q_{k_r}) \left(c_{0_r} + c_{1_r} \sum_{k_r} \tanh^2(q_{k_r}) + c_{2_r} \sum_{k_r \leq k'_r} \tanh^2(q_{k_r}) \tanh^2(q_{k'_r}) + \dots \right) \quad (6)$$

and

$$p_{\text{ext}} = \prod_{k_r} \text{sech}^2(q_{k_r}) \left(c_{0_r} + c_{1_r} \sum_{k_r} \tanh^2(q_{k_r}) + c_{2_r} \sum_{k_r \leq k'_r} \tanh^2(q_{k_r}) \tanh^2(q_{k'_r}) + \dots \right). \quad (7)$$

Finally, the fidelity of the heralded state to a single photon in the first spectral mode and vacuum in all other modes is

$$F = \langle 1_{0_r} | \otimes \langle 0_r | \rho | 1_{0_r} \rangle \otimes | 0_r \rangle = \frac{\prod_{k_r} \text{sech}^2(q_{k_r})}{p_{\text{herald}}} \frac{\prod_{k_r} \text{sech}^2(q_{k_r})}{p_{\text{ext}}} c_{1_r} c_{0_r} \tanh^2(q_{0_r}). \quad (8)$$

This is the fidelity of the heralded single photon before it is subjected to losses, upper bounding the possible performance of the source. This fidelity is plotted in figure 2, which shows the progression from an unfiltered, spectrally multimode state (with JSI matching our experiment), to filtered but contaminated with multiphoton events, to finally a high-fidelity state. An ideal photon source has simultaneously high heralding probability and fidelity, but without multiplexing heralded single photon sources are limited to the yellow region. Of course, one still wants to operate the sources as close to the upper right corner as possible. Here the unfiltered state shows consistently low fidelity, which can be increased by filtering, in our case to 50 GHz bandwidth. Without losses, the extended heralding case maintains high fidelity for significantly higher, as shown in the right plot of figure 2, heralding probability than the standard filtered case, approaching the theoretical limit much more closely.

It is unfortunately not possible to access this fidelity experimentally due to the difficulty of projecting on the vacuum and single photons in single spectral modes with realistic losses. The source quality can still be accessed, however, via the spectral purity P and heralded $g_h^{(2)}(0)$. Fidelity $F = 1$ corresponds to $P = 1$ and $g_h^{(2)}(0) = 0$. Here the purity is controlled by spectral filtering, which increases the $g_h^{(2)}(0)$ from pollution from other spectral modes, which is subsequently reduced by heralding plus feed-forward.

We now make a few approximations to express the fidelity equation (8) in terms of these experimentally accessible quantities. First we assume all q_{k_r} and $q_{k'_r}$ are small such that $\tanh(q_k) \approx q_k$ and $\text{sech}(q_k) \approx 1$. Then we neglect filtering (dropping the subscripts t), resulting in a fidelity

$$F \approx \frac{c_1 q_0^2}{p_{\text{herald}}}. \quad (9)$$

We then assume low overall generation probability and no dark counts, such that we can truncate p_{herald} to second order, giving

$$P_{\text{herald}} \approx c_1 \sum_k (q_k)^2 + c_2 \sum_{k \leq k'} (q_k)^2 (q_{k'})^2. \quad (10)$$

We expand the fidelity in a Taylor series about 0 in the second term of p_{herald} ($1/(a+x) \approx 1/a - x/a^2$), giving

$$F \approx \frac{q_0^2}{\sum_k (q_k)^2} \left(1 - \frac{c_2 \sum_{k \leq k'} (q_k)^2 (q_{k'})^2}{c_1 \sum_k (q_k)^2} \right). \quad (11)$$

The spectral purity is given in [41] as

$$P \approx \frac{\sum_k (q_k)^4}{(\sum_k (q_k)^2)^2} \approx \frac{q_0^4}{(\sum_k (q_k)^2)^2}, \quad (12)$$

where we assumed that the first Schmidt mode dominates, i.e. $q_0^4 \gg q_{k>0}^4$. Then we can identify this purity with the square of the first term in our approximate fidelity, resulting in

$$F \approx \sqrt{P} \left(1 - \frac{c_2 \sum_{k \leq k'} (q_k)^2 (q_{k'})^2}{c_1 \sum_k (q_k)^2} \right). \quad (13)$$

We similarly approximate and truncate the heralded state (equation (5)) to give

$$\rho_s \approx \frac{1}{P_{\text{herald}}} \left(c_1 \sum_k (q_k)^2 |1_k\rangle \langle 1_k| + c_2 \sum_{k \leq k'} (q_k)^2 (q_{k'})^2 |1_k, 1_{k'}\rangle \langle 1_k, 1_{k'}| \right). \quad (14)$$

The heralded $g_h^{(2)}(0)$ is given for multimode states [41] with broadband mode operators A_k by

$$g_h^{(2)}(0) = \frac{\left\langle \left(\sum_{j,m} A_j^\dagger A_m^\dagger A_j A_m \right) \right\rangle}{\left\langle \sum_j A_j^\dagger A_j \right\rangle^2}, \quad (15)$$

which when substituting ρ_s results in

$$g_h^{(2)}(0) \approx \frac{2c_2 P_{\text{herald}} \sum_{k \leq k'} (q_k)^2 (q_{k'})^2}{(c_1 \sum_k (q_k)^2)^2}. \quad (16)$$

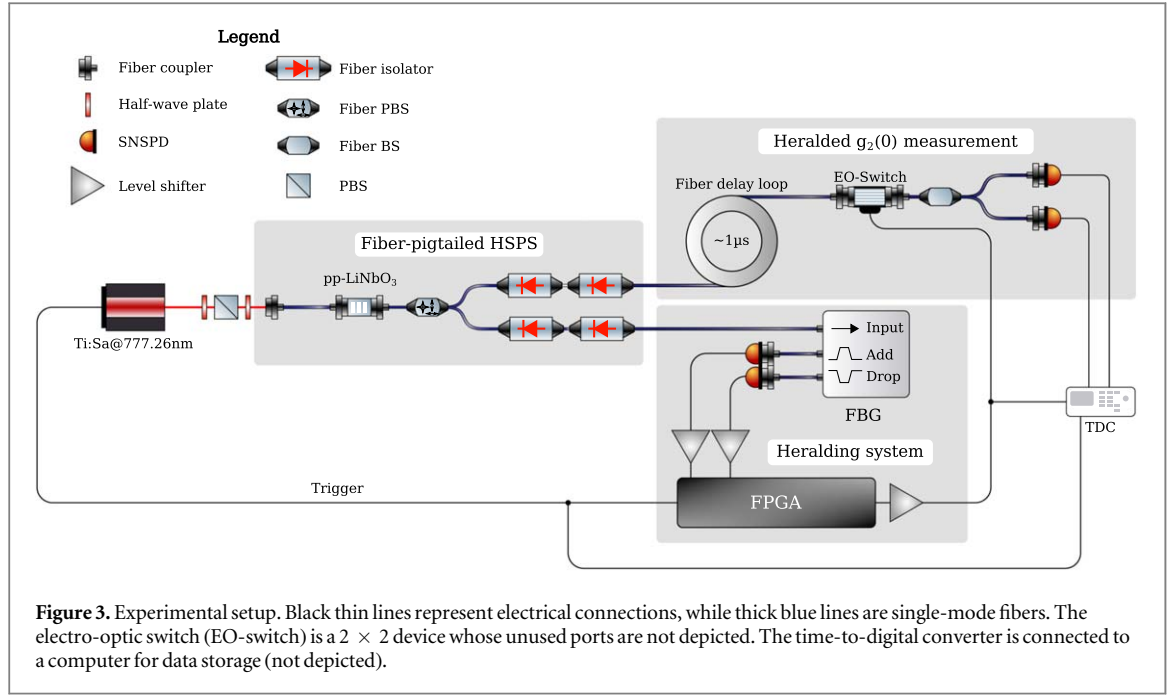
We then keep P_{herald} only to first order, allowing to identify the second term of our approximate fidelity with $g_h^{(2)}(0)/2$, resulting in

$$F \approx \sqrt{P} \left(1 - \frac{g_h^{(2)}(0)}{2} \right). \quad (17)$$

For the filtered case, with or without extended heralding, see the derivation in the [appendix](#), which shows equation (17) still holds. That is, the purity and $g_h^{(2)}(0)$ capture the relevant features (to first order) to measure the lossless heralded single-photon fidelity in cases of filtering, no filtering, and extended heralding.

2.2. Simulations

To characterize the efficacy of extended heralding in the presence of realistic spectral mode distributions, losses, and higher-order photon states, we performed numerical simulations using QuTiP [42]. We calculate the two-photon joint spectral amplitude of our photon pair source, perform a Schmidt decomposition to find the relative strengths of the involved squeezers, then normalize the overall pump power to give the appropriate total mean photon pair number. Next idealized (square, lossless) filters are applied to the heralding arm, and detector operations are applied to the transmitted and reflected arms, and we calculate the fidelity from (8). We also analyze the spectral purity and photon statistics via the $g_h^{(2)}(0)$ in order to compare with experiment. Finally we introduce the *heralded single-photon fitness* F_{HS} , so named because it captures two important aspects of a heralded single photon source: the presence of one photon in a single spectral mode upon heralding, and the absence of photons without heralding. The former is improved here by extended heralding, and the latter by using feedforward to control a physical switch on the heralded mode. The contributions of these terms are weighted by their likelihood. We define the heralded single-photon fitness as



$$\begin{aligned}
 F_{\text{HS}} &= p_{\text{herald}} F + (1 - p_{\text{herald}}) P_{\text{noclick}} \\
 &\approx p_{\text{herald}} \sqrt{P} \left(1 - \frac{g_h^{(2)}(0)}{2} \right) + (1 - p_{\text{herald}}) P_{\text{noclick}},
 \end{aligned} \tag{18}$$

where P_{noclick} is the probability of getting no detection in the heralded mode given that there was no heralding signal. This probability is also scaled to take into account losses in the setup, i.e.

$$P_{\text{noclick}} = 1 - \frac{P_{\text{click}}}{\eta}, \tag{19}$$

where η is the heralded photon's Klyshko efficiency, which gives the probability of producing no photon inside the source.

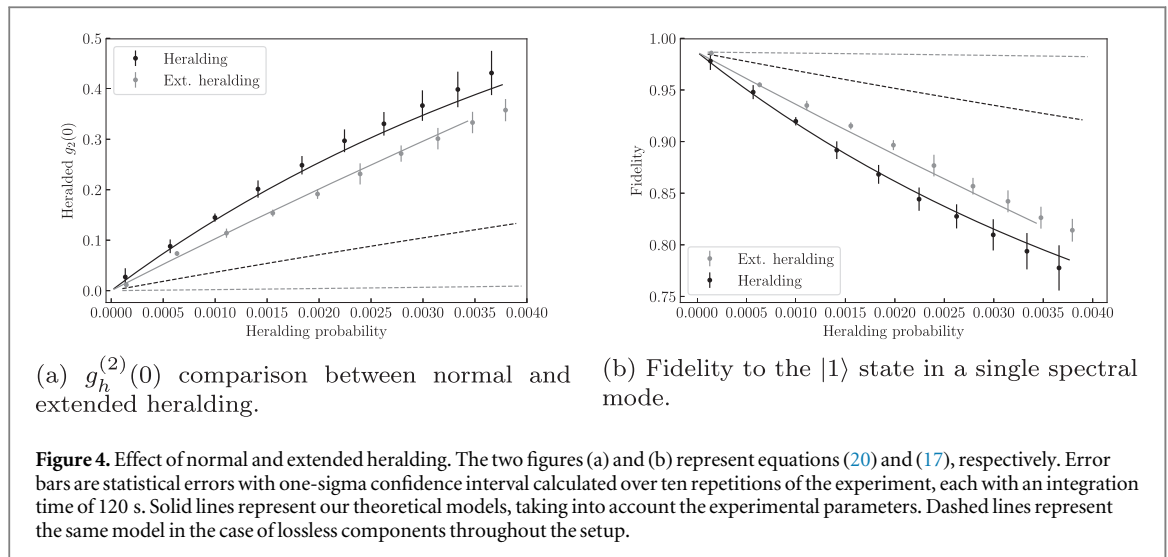
3. Experimental setup

The experimental setup is shown in figure 3. We use a type-II SPDC source based on a periodically-poled titanium-indiffused lithium-niobate waveguide. The source is fiber-pigtailed and is engineered to produce single photon pairs at 1560 nm when pumped at 780 nm and kept at room temperature [22]. However, in this experiment the source is kept at around 50 °C, to shift the degeneracy point of the source into a range that fits the window of the fiber Bragg-grating (FBG) filter used for heralding.

A pulsed laser system (*Spectra Physics Tsunami*) with a 2 ps bandwidth and centered at 777.24 nm with a repetition rate of 500 kHz pumps the SPDC and acts as the system clock. In order to control power and polarization of the pump, a half-wave plate, a polarizing beam-splitter, and a second half-wave plate, are placed just before light is coupled into the SPDC source. The pump is then coupled into a polarization maintaining fiber directly pigtailed to one of the end facets of the lithium-niobate chip. Photon pairs are then collected at the output end facet by another polarization maintaining fiber. The output fiber is fusion-spliced to a fiber polarizing beam-splitter to separate the two outputs of the source (typically called 'signal' and 'idler'). The outputs of the fiber PBS are then also spliced to two fiber isolators per arm to suppress the residual pump light. In our case, the signal arm is the one being filtered and the idler is the arm being analyzed.

The signal arm is connected to an FBG filter (*AOS Manual FBG*) centered at 1554.5 nm and with 0.25 nm bandwidth. The two outputs of the filter correspond to the selected portion of the spectrum we want to use for heralding ('add' or transmitted) and the extended-heralding one ('drop' or reflected).

To implement the schemes described above, we monitor both outputs of the filter and apply two different heralding criteria. In the first case, which we will use as benchmark and label simply 'heralding', the heralding signal is taken to be a click in the transmitted arm of the filter. In the second case, labeled extended heralding, the heralding signal is a combination of two events: a click in the transmitted arm and no clicks in the reflected arm. Additionally, in this second case the extended heralding signal is used to close an electro-optic switch. This



means that we are physically removing unheralded photons from the system instead of simply discarding such events during data-analysis, a feature which proves crucial in light sensitive applications.

In both cases, the signal arm photons are detected with a superconducting nanowire single-photon detector (SNSPD, *PhotonSpot*). The generated outputs are amplified to TTL levels and redirected to a field programmable gate-array (FPGA, *Xilinx Spartan 6*) which produces the final heralding signal, depending on the condition set. This signal is then fed to a time-to-digital converter (TDC, *AIT TTM 8000*) for analysis.

The idler arm is routed to a fiber loop which introduces a delay of approximately $1 \mu\text{s}$. This gives enough time for the electronics to generate the appropriate heralding signal as described above. This then is used to close an electro-optic switch, which is normally open (i.e. blocking transmission of the light). The output of the switch is then coupled to a non-polarizing beam-splitter, whose outputs are finally connected to two SNSPDs. Their outputs are analyzed by the TDC, which registers the timestamps of each detector click and saves them onto a computer.

4. Analysis and discussion

As stated before, filtering is the simplest way to improve the purity of a source with a correlated spectrum. This comes at a cost, namely a reduction in the generation rate of single-photons. To counteract this effect, the natural answer would be to increase the pump power used. This has the unwanted side-effect to also increase the multi-photon components of the final state. To show this behavior, we record the $g_h^{(2)}(0)$ value at different power levels when using the heralding signal from the transmitted FBG port. We show the data as a function of heralding probability as only the photons which have been heralded are usable. As summarized by figure 4(a), the $g_h^{(2)}(0)$ captures the undesired increase of the multiphoton-component contribution as the heralding probability increases. The $g_h^{(2)}(0)$ value is calculated according to

$$g_h^{(2)}(0) = \frac{C}{S_1 S_2} H, \quad (20)$$

where C is the number of heralded coincidences at the end of the non-polarizing beam-splitter, S_1 and S_2 are the heralded counts at each output, respectively, and H is the number of heralding signals in the experiment.

If we now take into account the reflected port of the FBG filter to generate the extended heralding signal, we can see that, for the same value of heralding probability, we have decreased the $g_h^{(2)}(0)$ value, indicating that we effectively mitigated the spurious contributions of multiple pairs. Additionally, the data is in good agreement with our theoretical model, which allows us to extrapolate the best possible improvement when sourcing components with lower losses.

Figures 4(a) and (b) show the measured values of the $g_h^{(2)}(0)$ and the fidelity, with the respective theoretical models. We can see that in each case theory and experiment are in good agreement, particularly for the solid lines, which directly implement in simulation the approximations made in the approximate fidelity equation (17). An additional consideration is that this scheme is more effective the harder the source is pumped, e.g. reaching a maximum improvement in $g_h^{(2)}(0)$ of 21%, or for the same $g_h^{(2)}(0)$, an improvement in the count rate of 1.2 times.

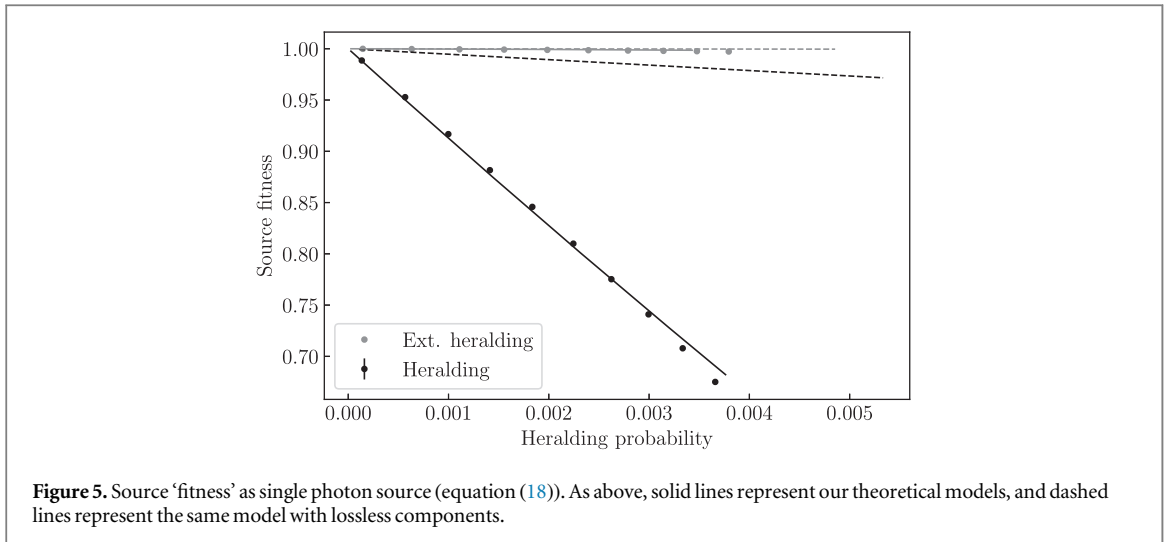


Figure 5. Source ‘fitness’ as single photon source (equation (18)). As above, solid lines represent our theoretical models, and dashed lines represent the same model with lossless components.

The performance of extended heralding is mainly limited by the losses in the experimental setup, as can be seen in the significant difference in the simulated curves with and without losses. Fiber-to-fiber connections, the FBG itself and the network connecting the source to the detection system all amount to an estimated 30% total transmission. Sourcing better components could increase the improvement obtained with this scheme over simple heralding to a more than 80% reduction in the $g_h^{(2)}(0)$.

In the previous two measurements, it is not necessary to implement feed-forward, as the same result can be achieved with post-selection. However, active gating is of importance when the total light flux reaching the experimental setup must be kept to a minimum, as it allows only correctly heralded photons to pass. The source fitness parameter F_{HS} as introduced in equation (18) directly captures this improvement, which cannot be achieved with post-selection, and gives us a quantitative measure of the noise reduction achieved thanks to this scheme. In contrast to the improvement in fidelity, here the increase in photon fitness is more significant for higher losses, as more losses in the heralding arm mean more unheralded events make it to the detectors without feed-forward. As seen in figure 5, the source fitness after extended heralding and feed-forward is nearly perfect, with a maximum improvement of 53%.

Another parameter used to characterize such active sources is the output noise factor (ONF) [35]. Given an heralding probability of 0.0037, optical switch on-time of 200 ns and optical switch extinction ratio of 20 dB, we calculated a ONF of $(2.4 \pm 2.0)\%$.

5. Conclusion

In this paper we have introduced and implemented a scheme called extended heralding, aimed at improving the standard filtering used to increase the spectral purity of photon pair sources with a correlated joint spectrum. A significant improvement is found when compared to a passive filter, especially when care is taken to minimize losses throughout the setup. This scheme is also easy to implement on top of an existing HSPS, requiring no modification of the existing setup. Finally we have demonstrated a significant reduction in unwanted incident light through the use of active feed-forward, which is important in practical light-sensitive scenarios.

Acknowledgments

The authors thank Johannes Tiedau for helpful discussions, and acknowledge support from the European Commission, European Research Council (ERC) (725366 QuPoPCoRN). EMS acknowledges support from the Natural Sciences and Engineering Research Council of Canada.

Appendix

Here we derive again the approximate fidelity in the filtering and extended heralding case, showing it gives the same result as equation (17). Again we assume all q_{k_i} and q_{k_r} are small such that $\tanh(q_k) \approx q_k$ and $\text{sech}(q_k) \approx 1$. Then the fidelity is

$$F \approx \frac{c_{1r} c_{0r} q_{0r}^2}{p_{\text{herald}} p_{\text{ext}}}. \quad (21)$$

We then assume low overall generation probability and no dark counts, such that we can truncate p_{herald} to second order, giving

$$p_{\text{herald}} \approx c_{1r} \sum_{k_t} (q_{k_t})^2 + c_{2r} \sum_{k_t \leq k'_t} (q_{k_t})^2 (q_{k'_t})^2, \quad (22)$$

and p_{ext} to first order as

$$p_{\text{ext}} \approx c_{0r} + c_{1r} \sum_{k_r} (q_{k_r})^2. \quad (23)$$

We also neglect the third-order term in the product $p_{\text{herald}} p_{\text{ext}}$, giving fidelity

$$F \approx c_{1r} c_{0r} q_{0r}^2 \left(c_{1r} c_{0r} \sum_{k_t} (q_{k_t})^2 + c_{2r} c_{0r} \sum_{k_t \leq k'_t} (q_{k_t})^2 (q_{k'_t})^2 + c_{1r} c_{1r} \sum_{k_t} (q_{k_t})^2 \sum_{k_r} (q_{k_r})^2 \right)^{-1}. \quad (24)$$

We then expand the fidelity in a Taylor series about 0 in the second two terms of the denominator ($1/(a+x) \approx 1/a - x/a^2$), giving

$$F \approx \frac{q_0^2}{\sum_{k_t} (q_{k_t})^2} \left(1 - \frac{c_{2r} c_{0r} \sum_{k_t \leq k'_t} (q_{k_t})^2 (q_{k'_t})^2}{c_{1r} c_{0r} \sum_{k_t} (q_{k_t})^2} - \frac{c_{1r} c_{1r} \sum_{k_t} (q_{k_t})^2 \sum_{k_r} (q_{k_r})^2}{c_{1r} c_{0r} \sum_{k_t} (q_{k_t})^2} \right). \quad (25)$$

The spectral purity is the same as before [41]

$$P \approx \frac{\sum_{k_t} (q_{k_t})^4}{\left(\sum_{k_t} (q_{k_t})^2 \right)^2} \approx \frac{q_0^4}{\left(\sum_{k_t} (q_{k_t})^2 \right)^2}. \quad (26)$$

We now include the reflected modes in the truncated heralded state (equation (5)) to give

$$\begin{aligned} \rho_s \approx & \frac{1}{p_{\text{herald}}} \left(c_{1r} \sum_{k_t} (q_{k_t})^2 |1_{k_t}\rangle \langle 1_{k_t}| + c_{2r} \sum_{k_t \leq k'_t} (q_{k_t})^2 (q_{k'_t})^2 |1_{k_t}, 1_{k'}\rangle \langle 1_{k_t}, 1_{k'}| \right) \\ & \otimes \frac{1}{p_{\text{ext}}} \left(c_{0r} |0\rangle \langle 0| + c_{1r} \sum_{k_r} (q_{k_r})^2 |1_{k_r}\rangle \langle 1_{k_r}| \right). \end{aligned} \quad (27)$$

The heralded $g_h^{(2)}(0)$ is given for multimode states [41] with broadband mode operators A_k by

$$g_h^{(2)}(0) = \frac{\left\langle \left(\sum_{j,m} A_j^\dagger A_m^\dagger A_j A_m \right) \right\rangle}{\left\langle \sum_j A_k^\dagger A \right\rangle^2}. \quad (28)$$

Substituting ρ_s and neglecting the reflected modes in the denominator results in

$$g_h^{(2)}(0) \approx \frac{2c_{2r} c_{0r} p_{\text{herald}} \sum_{k_t \leq k'_t} (q_{k_t})^2 (q_{k'_t})^2}{\left(c_{1r} c_{0r} \sum_{k_t} (q_{k_t})^2 \right)^2} + \frac{2c_{1r} c_{1r} p_{\text{herald}} \sum_{k_t} (q_{k_t})^2 \sum_{k_r} (q_{k_r})^2}{\left(c_{1r} c_{0r} \sum_{k_t} (q_{k_t})^2 \right)^2}. \quad (29)$$

The factor 2 comes from the annihilation operators themselves when they act on the same mode (i.e. $j = m = k_t = k'_t$), and from the two equivalent arrangements of annihilation operators when they act on different modes (e.g. $j = k_r, m = k_r$; or $j = k_r, m = k_t$). We then keep p_{herald} only to first order and assume negligible dark counts such that $c_{0r} \rightarrow 1$, allowing to identify the second term of our approximate fidelity with $g_h^{(2)}(0)/2$, resulting in the same fidelity as without filtering, namely

$$F \approx \sqrt{P} \left(1 - \frac{g_h^{(2)}(0)}{2} \right). \quad (30)$$

ORCID iDs

Marcello Massaro  <https://orcid.org/0000-0002-2539-7652>

Christine Silberhorn  <https://orcid.org/0000-0002-2349-5443>

References

- [1] Spring J B *et al* 2013 *Science* **339** 798–801
- [2] Tillmann M, Dakic B, Heilmann R, Nolte S, Szameit A and Walther P 2013 *Nat. Photon.* **7** 540–4
- [3] Crespi A, Osellame R, Ramponi R, Brod D J, Galvao E F, Spagnolo N, Vitelli C, Maiorino E, Mataloni P and Sciarrino F 2013 *Nat. Photon.* **7** 545–9
- [4] Carolan J *et al* 2015 *Science* **349** 711–6
- [5] Rudolph T 2017 *APL Photonics* **2** 030901
- [6] Azuma K, Tamaki K and Lo H K 2015 *Nat. Commun.* **6** 6787
- [7] Herbst T, Scheidl T, Fink M, Handsteiner J, Wittmann B, Ursin R and Zeilinger A 2015 *Proc. Natl Acad. Sci.* **112** 14202–5
- [8] Evans P G, Bennink R S, Grice W P, Humble T S and Schaake J 2010 *Phys. Rev. Lett.* **105** 253601
- [9] Tanzilli S, De Riedmatten H, Tittel W, Zbinden H, Baldi P, De Micheli M, Ostrowsky D and Gisin N 2001 *Electron. Lett.* **37** 26
- [10] Söller C, Cohen O, Smith B J, Walmsley I A and Silberhorn C 2011 *Phys. Rev. A* **83** 031806(R)
- [11] Fan J, Migdall A and Wang L J 2005 *Opt. Lett.* **30** 3368
- [12] Harada K, Takesue H, Fukuda H, Tsuchizawa T, Watanabe T, Yamada K, Tokura Y and Ichi Itabashi S 2011 *New J. Phys.* **13** 065005
- [13] Michler P, Kiraz A, Becher C, Schoenfeld W V, Petroff P M, Zhang L, Hu E and Imamoglu A 2000 *Science* **290** 2282–5
- [14] Shields A J 2007 *Nat. Photon.* **1** 215–23
- [15] Strauf S, Stoltz N G, Rakher M T, Coldren L A, Petroff P M and Bouwmeester D 2007 *Nat. Photon.* **1** 704–8
- [16] Alléaume R, Treussart F, Messin G, Dumeige Y, Roch J F, Beveratos A, Brouri-Tualle R, Poizat J P and Grangier P 2004 *New J. Phys.* **6** 92
- [17] Gaebel T, Popa I, Gruber A, Domhan M, Jelezko F and Wrachtrup J 2004 *New J. Phys.* **6** 98
- [18] Wu E, Rabeau J R, Roger G, Treussart F, Zeng H, Grangier P, Prawer S and Roch J F 2007 *New J. Phys.* **9** 434
- [19] Mosley P J, Lundeen J S, Smith B J, Wasylczyk P, U'Ren A B, Silberhorn C and Walmsley I A 2008 *Phys. Rev. Lett.* **100** 133601
- [20] Bruno N, Martin A, Guerreiro T, Sanguinetti B and Thew R T 2014 *Opt. Express* **22** 17246–53
- [21] Vergyris P, Kaiser F, Gouzien E, Sauder G, Lunghi T and Tanzilli S 2017 *Quantum Sci. Technol.* **2** 024007
- [22] Montaut N, Sansoni L, Meyer-Scott E, Ricken R, Quiring V, Herrmann H and Silberhorn C 2017 *Phys. Rev. Appl.* **8** 024021
- [23] Grice W P, U'Ren A B and Walmsley I A 2001 *Phys. Rev. A* **64** 063815
- [24] Pan J W, Bouwmeester D, Weinfurter H and Zeilinger A 1998 *Phys. Rev. Lett.* **80** 3891–4
- [25] Meyer-Scott E, Montaut N, Tiedau J, Sansoni L, Herrmann H, Bartley T J and Silberhorn C 2017 *Phys. Rev. A* **95** 061803(R)
- [26] Francis-Jones R J A, Hoggarth R A and Mosley P J 2016 *Optica* **3** 1270
- [27] Meany T, Ngah L A, Collins M J, Clark A S, Williams R J, Eggleton B J, Steel M J, Withford M J, Alibart O and Tanzilli S 2014 *Laser Photonics Rev.* **8** L42–6
- [28] Kaneda F, Christensen B G, Wong J J, Park H S, McCusker K T and Kwiat P G 2015 *Optica* **2** 1010
- [29] Joshi C, Farsi A, Clemmen S, Ramelow S and Gaeta A L 2018 *Nat. Commun.* **9** 847
- [30] Grimau Puigibert M, Aguilar G, Zhou Q, Marsili F, Shaw M, Verma V, Nam S, Oblak D and Tittel W 2017 *Phys. Rev. Lett.* **119** 083601
- [31] Ngah L A, Alibart O, Labonté L, D'Auria V and Tanzilli S 2015 *Laser Photonics Rev.* **9** L1–5
- [32] Rohde P P 2007 arXiv:quant-ph/0703238
- [33] Christ A and Silberhorn C 2012 *Phys. Rev. A* **85** 023829
- [34] Avella A *et al* 2011 *Opt. Express* **19** 23249
- [35] Brida G, Degiovanni I P, Genovese M, Migdall A, Piacentini F, Polyakov S V and Berchera I R 2011 *Opt. Express* **19** 1484–92
- [36] Brida G *et al* 2012 *Appl. Phys. Lett.* **101** 221112–4
- [37] Francis-Jones R J A and Mosley P J 2017 *J. Opt.* **19** 104005
- [38] Quesada N and Sipe J E 2015 *Phys. Rev. Lett.* **114** 093903
- [39] Christ A, Lupo C, Reichelt M, Meier T and Silberhorn C 2014 *Phys. Rev. A* **90** 023823
- [40] Brańczyk A M, Ralph T C, Helwig W and Silberhorn C 2010 *New J. Phys.* **12** 063001
- [41] Christ A, Laiho K, Eckstein A, Cassemiro K N and Silberhorn C 2011 *New J. Phys.* **13** 033027
- [42] Johansson J R, Nation P D and Nori F 2012 *Comput. Phys. Commun.* **183** 1760–72